DOI: 10.5281/zenodo.17075339

CHAPTER 3

Rare Earth Nanomaterials: Synthesis, Properties, and Emerging Applications

Sayantani Chall,[1*] Soumen Sarkar[2*]

[1]*School of applied science and humanities, Haldia Institute of Technology, Haldia, East Medinipur 721657 West Bengal, India*

[2]*Department of Chemistry, Balurghat College, Balurghat, South Dinajpur 733101 West Bengal, India*

Corresponding author Email: sayantani.chall@yahoo.com,[1] soumensarkar.chem1@gmail.com[2]

Received: 13 August 2025; Accepted: 02 September 2025; Available online: 08 September 2025

Abstract: Rare earth nanomaterials, derived from the unique *f*-block elements of the periodic table, have developed as a transformative class of functional nanomaterials with exceptional optical, magnetic, catalytic, and electronic properties. The partially filled *4f* orbitals endow these elements with sharp emission spectra, long fluorescence lifetimes, high magnetic anisotropy, and remarkable redox versatility, making them attractive for diverse applications in nanotechnology. This review presents a comprehensive overview of the strategies for synthesizing rare earth-based nanostructures, including doped nanocrystals, upconversion nanoparticles, and rare earth oxide or hydroxide nanomaterials. We examine the underlying structure–property relationships, highlighting how nanoscale engineering can modulate luminescence

Materials Science: Advances in Synthesis, Characterization and Applications (Vol. 1) - Digambar M. Sapkal, Harshal M. Bachhav, Gaurav Mahadev Lohar, Sanjay P. Khairnar (Eds.)

ISBN: 978-93-95369-55-8 (paperback) 978-93-95369-46-6 (electronic) | © 2025 Advent Publishing.

https://doi.org/10.5281/zenodo.17075339

efficiency, magnetic performance, and catalytic activity. Particular emphasis is placed on their role in bioimaging, photodynamic therapy, sensing, photocatalysis, and energy conversion technologies. The challenges of controlling size, morphology, surface chemistry, and biocompatibility are critically discussed alongside emerging solutions such as ligand engineering and hybrid nanocomposite design. Finally, we outline current trends and future prospects, emphasizing the potential of rare earth nanomaterials to bridge fundamental *f*-block chemistry with cutting-edge technological applications.

Keywords: Rare Earth Nanomaterials, Lanthanides, Soft Chemical Synthesis, Stability, Electrostatic Stabilization.

1. Introduction

The lanthanides are a series of fifteen metallic chemical elements in the periodic table, from atomic number 57 (lanthanum) to 71 (lutetium). Their general electron configuration is $[Xe]4f^{n-1}5d^{0-1}6s^2$, where n ranges from 1 to 15.[1,2] Research on lanthanide elements began in the 18th century, and over more than two hundred years, lanthanide chemistry has advanced significantly. The history of lanthanide discovery, beginning with the isolation of ytterbite in 1787 by Carl Axel Arrhenius, unfolded through over a century of painstaking chemical separations that enriched both inorganic chemistry and spectroscopy.[3] While their initial uses were limited, landmark innovations by Carl Auer von Welsbach in the late 19th and early 20th centuries established the first large-scale commercial applications of rare earth elements in lighting and ignition technologies. A defining feature of lanthanides-the sharp, well-resolved optical spectra arising from *f–f* transitions within shielded 4*f* orbitals-has since become central to a wide range of photonic technologies.

The integration of these rare earth elements into the nanoscale realm has given rise to lanthanide nanomaterials (LNMs), which combine the intrinsic luminescence, long-lived excited states, and high colour purity of lanthanides with size-dependent nanoscale effects.[4] Such materials are now indispensable in applications spanning catalysis, sensing, renewable energy, and biomedicine. In particular, lanthanide ions (Ln^{3+}) have proven invaluable in biological imaging and diagnostic assays due to the unique properties of open-shell *4f* electrons.[2] Their emission, extending from the visible to the near-infrared (NIR) range, offers optical signatures in spectral and temporal windows inaccessible to conventional probes. This enables applications in multiplexed disease diagnostics, deep tissue imaging in the NIR-II window (1000–1700 nm), and therapeutic interventions through bio-responsive activation of cellular pathways.[5,6]

Advances in nanofabrication have enabled the incorporation of luminescent lanthanides into diverse architectures, from molecular complexes and supramolecular assemblies to metal–organic frameworks (MOFs) and nanoparticles.[7,8] These nanoparticles—ranging from soft-matter systems to gold, silver, silica, and lanthanide-doped upconverting nanocrystals—offer platforms for both downconversion (DCNPs) and upconversion (UCNPs) luminescence, each with distinct advantages for bioimaging and

ISBN: 978-93-95369-55-8 (paperback) 978-93-95369-46-6 (electronic)

sensing.[9,10] By exploiting their tunable photophysical properties and compatibility with various host matrices, LNMs have become a hotspot of research at the intersection of nanotechnology, materials science, and biomedicine.[11-13] This review will provide a comprehensive overview of lanthanide nanomaterials, focusing mostly on their synthesis strategies and diverse applications.

2. Different Soft Chemical Synthesis Routes-Diverse Materials with Versatile Structures

The luminescent behaviour of Ln^{3+}-doped phosphors is strongly influenced by their composition, crystallinity, and structural features such as size and shape. Achieving tailored optical properties for luminescence and broader applications requires carefully chosen synthetic strategies. While traditional solid-state reactions at high temperatures have been used to prepare rare-earth-based phosphors, complex oxides, and sulfides, soft chemical routes have emerged as the preferred methods due to their precise control over particle morphology and surface chemistry.

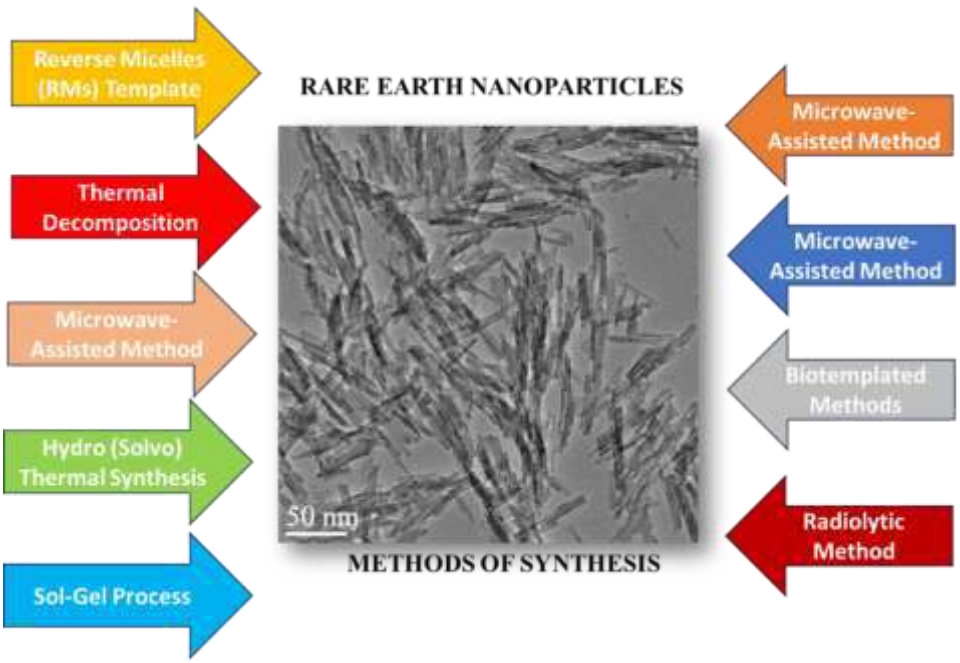

Fig. 1. The above figure demonstrates various soft chemical methods of rare earth nanomaterials synthesis. The transmission electron microscopy image represents formation of $LaPO_4$:Ce,Tb Nanorods via Ionic/Non-Ionic Reverse Micelle Templates.

Compared to solid-state synthesis, soft chemical approaches offer several advantages: (i) facile ligand introduction to prevent particle aggregation in aqueous or organic media; (ii) tunable parameters - raw materials, acidity, solvent, concentration, additives, temperature, and time - to control particle size and shape; (iii) low reaction temperatures, simple equipment, cost-effectiveness, scalability, and versatile post-treatment options.[14]

ISBN: 978-93-95369-55-8 (paperback) 978-93-95369-46-6 (electronic)

Common soft-chemical methods include surfactant-assisted micelles/reverse micelles, hydro/solvothermal synthesis, high-boiling solvent precipitation, sol–gel processing, bio-inspired synthesis, microwave-assisted techniques, ionic liquid-mediated reactions, and γ-radiolysis (Figure 1).

2.1 Reverse Micelles (RMs) Template

Reverse micelle (RM) templates are among the most versatile approaches for producing monodisperse nanoparticles. RMs are thermodynamically stable dispersions of nanosized surfactant aggregates in nonpolar solvents, with polar head groups facing inward and hydrocarbon tails outward. Water in the core ("water pool") is characterized by the molar ratio ω = [H_2O]/[surfactant], which directly affects droplet size.[15] Systems with ω < 15 are generally called reverse micelles, while higher ω values are termed microemulsions.[16]

These confined aqueous nanodomains dissolve reactants, and Brownian motion enables droplet exchange, creating nanoscale reactors for Ln^{3+}-based nanocrystal (NC) formation. Various water/surfactant/oil combinations e.g., water/CTAB/cyclohexane, water/CO520/cyclohexane, water/AOT/n-heptane have yielded YF_3, α/β-$NaYF_4$, Y_2O_3, CeF_3, ErF_3, and $LaPO_4$ up-/down-conversion NCs.[17,18] However, these often suffer from low yield and suboptimal crystallinity. To address this, Li et al.[19] developed an oil-in-water microemulsion route (hexane–linoleic acid–water), where reactions occur at the water–oil interface, producing highly passivated YF_3, PrF_3, NdF_3, $HoPO_4$, and $CePO_4$ NCs (1.5-5 nm). This method improves yield and productivity due to enhanced solubility of precursors in the aqueous phase.

2.2 Thermal Decomposition

Among soft-chemical routes, thermal decomposition is widely used to produce high-quality, monodisperse, highly crystalline, and phase-pure rare-earth (RE) nanoparticles (NPs) under 10 nm.[20] This oxygen-free organic-phase method involves dissolving RE organic salts—typically trifluoroacetates, oleates, acetylacetonates, or acetates—in high-boiling solvents such as octadecene (ODE, b.p. 315 °C) with coordinating surfactants like oleic acid (OA) and oleylamine (OM).[21] Surfactants cap NP surfaces to enhance dispersibility and prevent aggregation while controlling growth via selective adsorption. Yan *et al.* first synthesized OA-capped LaF_3 triangular nanoplates through shape-selective growth, while Capobianco *et al.*[22] and others optimized co-thermolysis of trifluoroacetates in solvents (OM, OA/ODE, OA/OM, OA/OM/ODE) to prepare Ln^{3+}-doped fluoride nanocrystals (NCs) with diverse morphologies.[23,24] Murray *et al.*[25] demonstrated size- and shape-controlled synthesis of uniform hexagonal RE fluoride NPs, and Chen *et al.*[26-27] developed a low-toxicity approach using $RE(OA)_3$ complexes. Morphology and size are strongly influenced by reaction temperature, time, and OA content.[29,30]

Despite its advantages, this method requires stringent anhydrous, oxygen-free, high-temperature conditions; uses costly solvents; and produces toxic by-products from trifluoroacetates. Products are typically hydrophobic due to surfactant capping, necessitating surface modification for bioapplications,

ISBN: 978-93-95369-55-8 (paperback) 978-93-95369-46-6 (electronic)

and it is unsuitable for RE phosphates, vanadates, and borates, with limited morphology control for $LnPO_4$. Additionally, the NP formation mechanism remains unclear, hindering precise design.

2.3. Co-Precipitation Method

The coprecipitation method is among the earliest and most practical strategies for preparing Ln^{3+}-doped nano- and microcrystals, owing to its mild conditions, straightforward procedures, and low-cost equipment requirements. The initial approach was introduced by van Veggel and colleagues, who synthesized sub-10 nm LaF_3:Ln (Ln = Eu, Er, Nd, Ho) nanoparticles via coprecipitation of RE^{3+} and F^- ions in an ethanol–water medium at 75 °C, using ammonium di-n-octadecyldithiophosphate as a capping ligand to regulate particle growth, prevent aggregation, and enhance dispersibility in organic solvents.[31,32] Following a similar strategy, YVO_4 nanoparticles (5–10 nm) were obtained by substituting F^- with VO_4^{3-} ions.[33]

Van Veggel's group later reported the synthesis of water-dispersible LnF_3 (Ln = La, Ce, Nd, Eu, Gd) and NaxLnyFz (Ln = Gd, Dy–Er, Yb) nanoparticles (3–10 nm) using NH_4OH-neutralized citric acid as a stabilizer at 75 °C, with citrate ligands significantly improving the aqueous solubility of the products.[34] Yi *et al*.[35] subsequently demonstrated the room-temperature synthesis of RE nanocrystals using ethylenediaminetetraacetic acid (EDTA) as a chelating agent, where tuning the EDTA/RE^{3+} molar ratio from 0 to 1.5 reduced particle size from 166 nm to 37 nm.[36] The morphology of the resulting nanoparticles was found to be highly sensitive to pH.

Coprecipitation has also been applied to the fabrication of hollow nano- and microspheres by employing sacrificial templates such as silica, carbon, polystyrene, or melamine-formaldehyde. Using this approach, hollow Ln^{3+}-doped LaF_3, YVO_4, and RE_2O_3 (RE = La, Gd, Lu, Y) structures have been successfully synthesized.[37] However, this method generally yields products with simple and coarse morphologies that are challenging to fine-tune. Furthermore, as-synthesized particles typically exhibit weak luminescence, requiring post-annealing to improve emission intensity. The annealing process, however, often removes capping ligands such as EDTA, reducing hydrophilicity and thereby limiting applications in biological systems unless additional surface modifications are introduced.

Despite these drawbacks, coprecipitation remains highly relevant for industrial-scale applications because of its advantages in terms of high yield, low cost, environmental compatibility, and overall ease of synthesis.

2.4. Hydro (Solvo) Thermal Synthesis

The solvothermal method, widely applied since the mid-1990s, employs solvents under high pressure and elevated temperatures in sealed Teflon-lined autoclaves to accelerate reactions between solids. This environment enhances solubility and reactivity, enabling processes not feasible at atmospheric pressure, and often operates above the solvent's critical point, providing flexibility in designing high-quality inorganic materials. For rare-earth (RE) compounds, common precursors include nitrates or chlorides, with fluoride sources such as HF, NH_4F, NaF, and $NaBF_4$; phosphate, vanadate, molybdate, tungstate, and

ISBN: 978-93-95369-55-8 (paperback) 978-93-95369-46-6 (electronic)

borate sources include $Na_3PO_4/(NH_4)_2HPO_4/(NH_4)H_2PO_4$, $Na_3VO_4/(NH_4)_3VO_4$, $Na_2MoO_4/(NH_4)_2MoO_4$, Na_2WO_4, and HBO_3. Solvents like water, ethanol, and ethylene glycol influence morphology and size through their physicochemical properties. Organic additives or surfactants such as oleic acid (OA),[38] polyethyleneimine (PEI),[39,40] EDTA,[41.42] and CTAB are often included for simultaneous control over phase, size, shape, and surface functionalization. Li *et al.*[43] introduced a multiphase, interface-controlled liquid-solid-solution (LSS) strategy enabling monodisperse, high-crystallinity Ln^{3+}-doped NPs with tailored properties, leading to successful syntheses of $NaYF_4$,[44-46] $NaLaF_4$,[47] $NaLuF_4$,[48,49] $BaGdF_5$,[50] YF_3,[51] LaF_3,[52,53] LaOF,[54,55] GdF_3,[56] CaF_2,[57] SrF_2,[58] BaF_2,[59] and $KMnF_4$.[60]

2.5. Sol-Gel Process

The sol–gel process, a soft-chemical route for fabricating Ln^{3+}-doped nanocrystals (NCs), involves forming inorganic/organic networks in solution at low temperatures, transitioning from sol to gel, followed by high-temperature calcination to achieve pure-phase, highly crystalline multicomponent NCs with strong luminescence. Prasad *et al.* developed an emulsion-based variant, the sol–emulsion–gel method.[61,62] In the Pechini-type sol–gel method, aqueous metal salt precursors (nitrates, chlorides, acetates) are complexed with hydroxycarboxylic acids (e.g., citric or salicylic acid), then polyesterified with polyhydroxy alcohols (e.g., PEG, EG) to form homogeneous polymeric gels, minimizing ion segregation and ensuring compositional uniformity. Calcination at 500–1000 °C yields pure-phase NCs such as LaOCl:Ln (Ln = Dy, Tb), $CaInO_4$:Eu, $LaAlO_3$:Ln (Ln = Tm, Tb), $LaGaO_3$:Ln (Ln = Sm, Tb), and $CaYAlO_4$:Ln (Ln = Eu, Tb).[63-65] However, high annealing temperatures can cause aggregation, irregular morphologies, and broad size distributions. Core–shell structures (300 nm–1.2 μm) such as SiO_2@Y_2O_3:Eu, SiO_2@YVO_4:Eu, SiO_2@$LaPO_4$:Ce,Tb, SiO_2@YBO_3:Eu, SiO_2@$CaWO_4$:Ln (Ln = Eu, Tb), and SiO_2@$CaMoO_4$:Tb have also been synthesized,[66-67] with shell thickness controlled by deposition cycles (typically 30–100 nm per cycle). These core–shell phosphors maintain perfect sphericity, narrow size distribution, non-agglomeration, and smooth surfaces even after four coatings.

2.6. Microwave-Assisted Method

Over the past three years, the microwave-assisted method has gained significant attention for its ability to reduce reaction times from several hours to just minutes. This efficiency arises from in-core volumetric heating induced by microwave radiation, which directly heats the sample.[68] Compared with conventional thermal methods, microwave dielectric heating offers rapid and uniform heating, solvent superheating, and selective heating effects.[69] As a result, it has emerged as an energy-efficient and versatile approach for synthesizing nanoscale inorganic materials. For instance, Zhang et al. synthesized hydrophilic $BaYF_5$:Ce,Tb and MF_2:Ln (M = Ca, Sr, Ba; Ln = Ce, Tb, Gd) nanocrystals within 10 minutes using ethylene glycol as solvent. Similarly, Lin and co-workers reported the microwave-assisted preparation of $CePO_4$:Tb nanorods, Ln^{3+}-doped $NaGdF_4$ UCNPs, and $NaYF_4$:Yb,Ln (Ln=Er, Tm, Ho) nanocrystals/microcrystals within 10 minutes to 3 hours.[70]

ISBN: 978-93-95369-55-8 (paperback) 978-93-95369-46-6 (electronic)

2.7. Ionic-Liquids Based Synthesis

Ionic liquids (ILs) are nonvolatile, nonflammable, thermally stable organic salts, often termed "green solvents" due to their low melting points (<100 °C), tunable polarity, wide electrochemical window, and ability to dissolve and stabilize metal cations, enabling their use as solvents, capping agents, or surfactants in inorganic synthesis.[71] They have proven particularly effective for rare-earth fluoride nanomaterials, as counterions such as $[BF_4]^-$, $[BF_6]^-$, and $[PF_6]^-$ can decompose or hydrolyze to release F^- ions under suitable conditions.[72,73] Using this property, hydrophilic LnF_3 (Ln = La–Nd, Sm, Eu, Tb, Er) nanocrystals have been synthesized by precipitation of rare-earth salts in ILs like [Bmim][BF_4], [Bmim][PF_6], [Omim][PF_6], and [Omim][BF_4], where the IL served as solvent, template, and fluorine source.[74,75] Similarly, $NaYF_4$:Yb,Er/Tm nanoparticles have been prepared via solvothermal methods with [Bmim][BF_4] acting as solvent, co-solvent, reactant, and template.[76] More recently, microwave-assisted IL synthesis has yielded diverse morphologies (nanodisks, nanoclusters, elongated nanoparticles) within 5–20 min, benefiting from the strong microwave-absorbing ability of ILs to produce highly crystalline products efficiently.[77]

2.8. Biotemplated Methods

Biological materials possess intricate nanostructures often beyond the reach of current synthetic techniques, making biological scaffolds attractive for designing advanced nanomaterials. While lanthanide-based nanocrystals offer strong luminescence, their limited water solubility and biocompatibility have hindered biological applications. Wang *et al.*[78] achieved one-pot synthesis of chitosan-capped LaF_3:Eu^{3+} nanocrystals (~20 nm) that are water-soluble, biocompatible, highly fluorescent, and stable in pH 2–7.4. Chitosan provided hydroxyl and amino groups for biomolecule conjugation, enabling uses such as intracellular labeling. Zhou *et al.* [79] developed a DNA-guided approach for $NaGdF_4$:Ce/Tb nanoparticles, where residual DNA from synthesis served as a biotemplate for $CaPO_4$ nucleation, creating a pH-responsive theranostic platform. Further aptamer functionalization enhanced targeted cellular uptake via receptor-mediated endocytosis.

2.9. Radiolytic Method

Radiolytic synthesis is a versatile technique offering controlled metal ion reduction via solvated electrons and secondary radicals, avoiding extraneous reagents and enabling reactions at room temperature.[80] Pioneering work by Belloni[81,82] and Henglein[83] utilized γ-radiation for preparing metal nanoparticles, leveraging hydrated electrons as powerful reducing agents ($E^0(H_2O/e^-_aq)$ = –2.87 V_NHE; $E^0(H^+/H)$ = –2.3 V_NHE). Examples include Au nanorods in CTAB,[84] Ag–Pt bimetallic nanoparticles,[85] Ag–polyaniline core–shell nanocomposites,[86] bimetallic nanoclusters,[87,88] cysteine-capped CdS NPs,[89] Ni clusters on α-Al_2O_3,[90] and noble metal clusters in silica aerogels.[91] Although less explored for rare-earth systems, Cuba et al.[92] reported γ-radiation synthesis of yttrium aluminium garnet, and Barta et al.[93] prepared cerium-doped lutetium aluminium garnet via this approach.

ISBN: 978-93-95369-55-8 (paperback) 978-93-95369-46-6 (electronic)

2. Fundamental factors controlling growth of rare earth nanostructures

Nucleation marks the onset of a phase transition within a localized region of a medium. Typically, it occurs at specific nucleation sites such as surfaces in contact with a liquid or vapor phase. In many cases, suspended particles or microscopic bubbles can also act as nucleation centres, a process referred to as heterogeneous nucleation. In contrast, homogeneous nucleation arises spontaneously in the absence of preferential sites, but requires conditions of superheating or supercooling to initiate.

In the context of nanotechnology, nucleation corresponds to the initial generation of small crystallites during precipitation. These early crystallites rapidly aggregate, progressing toward larger and more thermodynamically stable particles—a process known as nanoparticle growth. The interplay between nucleation and subsequent growth is a primary determinant of the final particle size and morphology. Experimental studies indicate that most precipitation reactions are governed by diffusion-controlled kinetics. The growth rate (G) of nanoparticles can be described by the relation $G = k_G \cdot S^g$, where k_G represents the growth rate constant, g the growth order, and S the degree of supersaturation. Supersaturation is given by $S = (a_A + a_B)/K_{sp}$, where a_A and a_B are the solute activities of species A and B, and K_{sp} is the solubility product constant.

A critical factor in regulating colloidal nanocrystal growth is the presence of stabilizers-molecular species that adsorb dynamically to the nanoparticle surface during synthesis. Stabilizers must balance two competing requirements: they must be sufficiently mobile to allow monomer addition to the growing crystal, yet stable enough to prevent uncontrolled aggregation. Strongly binding stabilizers can excessively hinder growth, while weakly coordinating molecules may lead to uncontrolled particle enlargement or aggregation. Examples of effective stabilizers include alkyl thiols, phosphines, phosphine oxides, phosphates, phosphonates, amides, amines, carboxylic acids, and aromatic nitrogen compounds. In addition, biocompatible polymers, peptides, proteins, and nucleic acids have also been widely employed as stabilizing agents.[94,95]

Stabilization strategies are broadly divided into electrostatic stabilization and steric stabilization.[96] In electrostatic stabilization, adsorption of ionic stabilizers onto the nanoparticle surface generates an electrical double layer, leading to Coulombic repulsion that prevents aggregation (Figure 2a). However, this method has limitations: it provides only kinetic stability, is effective mainly in dilute systems, is sensitive to electrolytes, and fails to redisperse aggregated particles.[97]

By contrast, steric stabilization (Figure 2b) involves surrounding nanoparticles with bulky molecular layers, such as polymers or surfactants, which create a steric barrier to aggregation.[98] Unlike electrostatic stabilization, steric stabilization offers thermodynamic stability, ensuring that dispersions remain redispersible, unaffected by electrolytes, and capable of supporting high particle concentrations.

Thus, controlling nucleation, growth kinetics, and stabilization mechanisms is essential to tailoring the size, morphology, and dispersibility of rare earth nanostructures, which ultimately governs their functional properties.

ISBN: 978-93-95369-55-8 (paperback) 978-93-95369-46-6 (electronic)

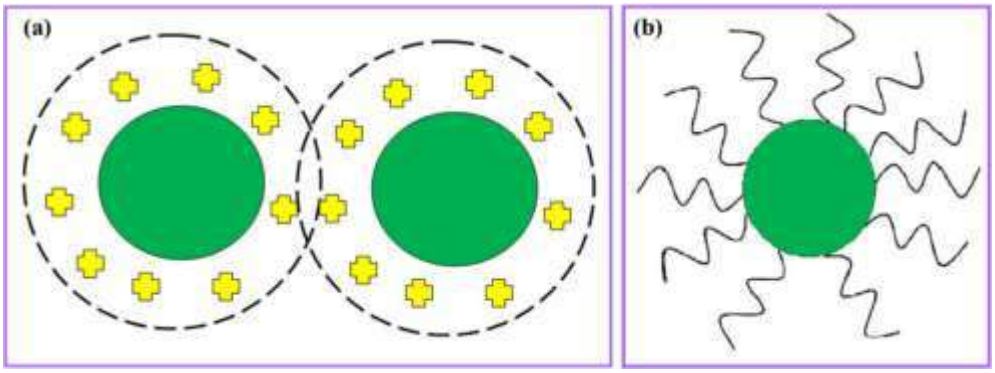

Fig. 2. Pictorial representation of (a) Electrostatic stabilization of particles and (b) steric stabilization of particles.

3. Applications of rare earth nanomaterials

Lanthanide nanomaterials are considered as highly promising materials in different applications arena (Figure 3). Lanthanide-doped nanoparticles (e.g., $NaYF_4$: Yb^{3+}/Er^{3+}) display sharp emissions, long lifetimes, and resistance to photobleaching—making them excellent for high-contrast biological imaging and biosensing. Their ability to absorb near-infrared (NIR) light reduces autofluorescence and enhances tissue penetration.[99] Engineered UCNPs serve dual roles in fluorescence imaging and phototherapy. One study created UCNP@Au nanostructures for NIR imaging and photothermal treatment of glioma cells; another design combined UCNP cores with mesoporous silica and a pH-responsive gatekeeper for targeted drug delivery.[100] Rare-earth upconversion nanomaterials enable deep-tissue PDT by converting NIR to visible light to drive photosensitizer activation while minimizing tissue damage.[101] **(**Er^{3+}/Yb^{3+}-doped UCNPs have been used as intracellular nanothermometers, resolving temperature differences below 0.5 °C in live cells based on ratiometric emission analysis.[102] Their multiplexed luminescence further supports sensing heavy metals and biomolecules in complex environments. UCNPs emitting blue light under NIR excitation have enabled non-invasive neural control in live animals, including deep-brain stimulation and seizure suppression. Lanthanide-doped nanophosphors, prized for their photochemical stability, serve as sensitive probes for environmental monitoring and detection of hazardous ions like Hg^{2+} or Fe^{3+}.[103] Rare earth fluorescent nanomaterials such as YVO_4:Eu and $LaPO_4$:Ce,Tb have been successfully applied in forensic science, highlighting latent fingerprints with high contrast and minimal background interference.[104] Rare earth nanomaterials' narrow emission bands and low toxicity make them suitable for electrochemical sensors, supercapacitors, batteries, and catalysis (e.g., hydrogen evolution reaction).[105] Though not exclusive to rare earths, luminescent solar concentrators using rare-earth-based emitters have shown promise in enhancing building-integrated photovoltaics through efficient light collection and emission tuning. Rare earth nanomaterials enhance bone formation by promoting stem cell proliferation, differentiation, collagen production, and mineralization. They also modulate immune response and angiogenesis to support regenerative microenvironments.[106] Emerging layered nanostructures—like rare earth hydroxides and perovskites-have shown potential in MRI and drug delivery applications due to their flexibility, high surface area, and superlattice-forming capabilities.[107] Er-

ISBN: 978-93-95369-55-8 (paperback) 978-93-95369-46-6 (electronic)

doped WS_2 nanosheets integrated with silicon heterojunctions demonstrate both up- and down-conversion photoluminescence, offering high photoresponsivity (~39.8 mA/W) and potential paths toward advanced IR sensors.[108] Rare earth-based materials—particularly when paired with transition metals-are being investigated for magnetic sensors and memory technologies. Their tunable electronic and magnetic properties are promising for emerging spintronic applications like MRAM).[109] Intrinsic ferromagnetic semiconductors within the rare-earth nitride family show promise for cryogenic electronic devices, offering novel properties at low temperatures.

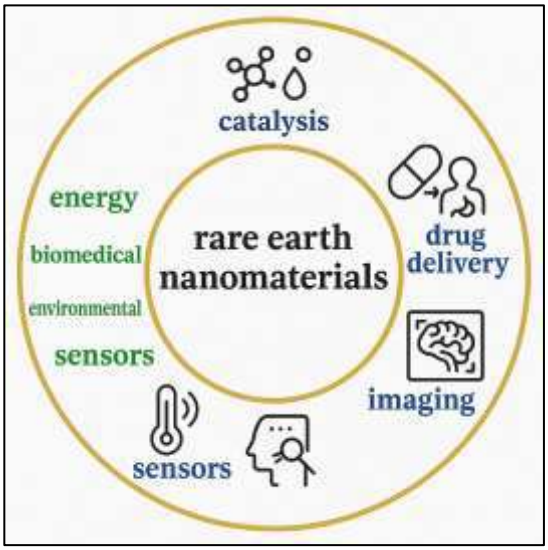

Fig. 3. The figure above illustrates manifold applications of rare earth nanomaterials in the diverse fields. Specific examples have been discussed in the text.

4. Future perspectives and Conclusion

Rare earth nanomaterials have demonstrated remarkable progress in their controlled synthesis, tunable properties, and versatile applications spanning photonics, catalysis, biomedicine, and energy systems. However, despite these advances, several challenges remain that must be addressed to unlock their full potential. One critical direction is the development of greener and scalable synthetic strategies that minimize the use of hazardous reagents and energy-intensive processes, enabling environmentally sustainable production at an industrial scale. Additionally, achieving precise control over size, morphology, dopant distribution, and surface chemistry is essential to bridge the gap between laboratory-based demonstrations and real-world applications.

In terms of properties, future work should focus on understanding the structure–property relationships at the nanoscale, particularly how dopant concentration, surface defects, and ligand chemistry influence luminescence efficiency, catalytic activity, and magnetic behaviour. Advanced in-situ characterization tools and computational modelling will play a vital role in unravelling these mechanisms, allowing rational design of next-generation rare earth nanostructures.

ISBN: 978-93-95369-55-8 (paperback) 978-93-95369-46-6 (electronic) | © 2025 Advent Publishing.

The emerging applications of these materials in bioimaging, drug delivery, quantum technologies, and renewable energy conversion highlight their transformative potential. Yet, issues of biocompatibility, toxicity, and long-term stability must be systematically studied to ensure safe integration into biomedical and environmental systems. Furthermore, coupling rare earth nanomaterials with hybrid platforms such as plasmonic nanostructures, 2D materials, and metal–organic frameworks (MOFs) open exciting avenues for multifunctional devices.

Conclusively, rare earth nanomaterials stand at the forefront of nanoscience and technology, with their unique optical, electronic, and magnetic properties driving innovation across disciplines. Continued advances in synthesis, mechanistic understanding, and functional integration will be crucial to realizing their promise in sustainable energy, advanced healthcare, and emerging quantum applications. With interdisciplinary efforts, these nanomaterials are poised to play a central role in shaping the next generation of high-performance materials and technologies.

Acknowledgement: Author S.C acknowledges Haldia Institute of Technology, Haldia, West Bengal and author S.S acknowledges Balurghat College, Dakshin Dinajpur, West Bengal.

References

1. J.C.G. Bünzli, and C. Piguet, *Chem. Soc. Rev.,* 2005, 34, 1048.
2. H. Dong, S.R. Du, X.Y. Zheng, G.M. Lyu, L.D. Sun, L.D. Li, P.Z. Zhang, C. Zhang, and C.H. Yan, *Chemical reviews*, 2015, 115, 19 ,10725-10815.
3. L. Eyring, K.A. Gschneidner, and G.H. Lander, *Handbook on the physics and chemistry of rare earths, Elsevier,* 2002, (Vol. 32).
4. C. Alexander, Z. Guo, P.B. Glover, S. Faulkner and Z. Pikramenou, *Chemical Reviews*, 2025, 125(4), 2269-2370.
5. S. Ali, W. Hou, Z. Wang and Y. Song, *Langmuir*. 2025.
6. L. Zou, Z.H. Chen, R. Fang, X. Liu, K. Xu, J. Ding, J. Wang, F. Zhang, Y. Fang and H., Tian, *ACS nano*, 2025, 19, 11, 10966-10976.
7. C. Alexander, Z. Guo, P.B. Glover, S. Faulkner, and Z. Pikramenou, *Chemical Reviews*, 2025, 125, 4, 2269-2370.,
8. S.N. Zhao, G. Wang, D. Poelman, and P.V.D. Voort, *Materials*, 2018, 11, 4, 572.
9. J.F.C. Loo, Y.H. Chien, F. Yin, S.K. Kong, H.P. Ho, and K.T. Yong, *Coordination Chemistry Reviews,* 2019, 400, 213042.
10. C. Cao, Q. Liu, M. Shi, W. Feng, and F. Li, *Inorganic chemistry*, 2019, 58,14, 9351-9357.

ISBN: 978-93-95369-55-8 (paperback) 978-93-95369-46-6 (electronic) | © 2025 Advent Publishing.

11. N.N. Nam, T.N.D. Trinh, H.D.K. Do, T.B. Phan, K.T.L. Trinh, and N.Y. Lee, *Spectrochimica Acta Part A: Molecular and Biomolecular Spectroscopy*, 2025, 327,125347.
12. Z. Li, J. Gong, S. Lu, X. Li, X. Gu, J. Xu, J.U. Khan, D. Jin, and X. Chen, *BMEMat,* 2024, 2, 4,12088.
13. A.K. Singh, *Coordination Chemistry Reviews*, 2022, 455, 214365.
14. S. V. Eliseevaab and J. -C. G. Bünzli, *New J. Chem.*, 2011, 35, 1165.
15. S. Gai, C. Li, P. Yang and J. Lin, *Chem. Rev.*, 2014, 114, 2343.
16. A. K. Ganguli, A. Ganguly and S. Vaidya, *Chem. Soc. Rev.*, 2010, 39, 474.
17. M. P. Pileni, *J. Phys. Chem. C*, 2007, 111, 9019.
18. H. Huang, G. Q. Xu, W. S. Chin, L. M. Gan and C. H. Chew, *Nanotechnology*, 2002, 13, 318.
19. P. Ghosh and A. Patra, *J. Phys. Chem. C*, 2008, 112, 3223.
20. J. -P. Ge, W. Chen, L. -P. Liu and Y. -D. Li, *Chem. Eur. J.*, 2006, 12, 6552.
21. G. Chen, T. Y. Ohulchanskyy, R. Kumar, H. Ågren and P. N. Prasad, *ACS Nano*, 2010, 4, 3163.
22. S. Mourdikoudis and L. M. Liz-Marzan, *Chem. Mater.*, 2013, 25, 1465.
23. N. Bogdan, F. Vetrone, G. A. Ozin and J. A. Capobianco, *Nano Lett.*, 2011, 11, 835.
24. G. S. Yi and G. M. Chow, *Adv. Funct. Mater.*, 2006, 16, 2324.
25. G. S. Yi and G. M. Chow, *J. Mater. Chem.*, 2005, 15, 4460.
26. C. Liu, H. Wang, X. Zhang and D. Chen, *J. Mater. Chem.*, 2009, 19, 489.
27. C. Liu, H. Wang, X. Li and D. Chen, *J. Mater. Chem.*, 2009, 19, 3546.
28. Y. Wei, F. Lu, X. Zhang and D. Chen, *Chem. Mater.*, 2006, 18, 5733.
29. Z. Li and Y. Zhang, *Nanotechnology*, 2008, 19, 345606.
30. F. Shi, J. Wang, D. Zhang, G. Qin and W. Qin, *J. Mater. Chem.*, 2011, 21, 13413.; J. W. Stouwdam and F. C. J. M. van Veggel, *Nano Lett.*, 2002, 2,733.
31. V. Sudarsan, F. C. J. M.van Veggel, R. A. Herring and M. Raudsepp, *J. Mater. Chem.*, 2005, 15, 1332.
32. J. W. Stouwdam, M. Raudsepp and F. C. J. M. van Veggel, *Langmuir*, 2005, 21, 7003.
33. F. Evanics, P. R. Diamente, F. C. J. M. van Veggel, G. J. Stanisz and R. S. Prosser, *Chem. Mater.*, 2006, 18, 2499.
34. G. Yi, H. Lu, S. Zhao, Y. Ge, W. Yang, D. Chen and L. -H. Guo, *Nano Lett.*, 2004, 4, 2191.

ISBN: 978-93-95369-55-8 (paperback) 978-93-95369-46-6 (electronic)

35. Y. Wei, F. Lu, X. Zhang and D. Chen, *J. Alloys Compd.*, 2007, 427, 333.
36. G. Jia, K. Liu, Y. Zheng, Y. Song and H. You, *Cryst. Growth Des.*, 2009, 9, 3702.
37. Z. Xu, Y. Gao and J. Lin, *J. Mater. Chem.*, 2012, 22, 21695.
38. H. -X. Mai, Y. -W. Zhang, L. -D. Sun and C. -H. Yan, *J. Phys. Chem. C*, 2007, 111, 13721.
39. F. Wang, X. Fan, M. Wang and Y. Zhang, *Nanotechnology*, 2007, 18, 025701.
40. F. Wang, R. Deng, J. Wang, Q. Wang, Y. Han, H. Zhu, X. Chen and X. Liu, *Nat. Mater.*, 2011, 10, 968.
41. R. Komban, K. Koempe and M. Haase, *Cryst. Growth Des.*, 2011, 11, 1033.
42. Z. Xu, C. Li, D. Yang, W. Wang, X. Kang, M. Shang and J. Lin, *Phys. Chem. Chem. Phys.*, 2010, 12, 11315.
43. Z. Xu, C. Li, G. Li, R. Chai, C. Peng, D. Yang and J. Lin, *J. Phys. Chem. C*, 2010, 114, 2573.
44. G. Jia, H. You, Y. Song, J. Jia, Y. Zheng, L. Zhang, K. Liu and H. Zhang, *Inorg. Chem.,* 2009, 48, 10193.
45. Y. Zeng, Z. Li, L. Wang and Y. Xiong, *Cryst. Eng. Comm.*, 2012, 14,7043.
46. X. Liu and J. Lin, *J. Mater. Chem.*, 2008, 18, 221.
47. G. Li, C. Li, C. Zhang, Z. Cheng, Z. Quan, C. Peng and J. Lin, *J. Mater. Chem*., 2009, 19, 8936.
48. G. Li, Z. Hou, C. Peng, W. Wang, Z. Cheng, C. Li, H. Lian and J. Lin, *Adv. Funct. Mater*., 2010, 20, 3446.
49. F. Wang, X. Xue and X. Liu, *Angew. Chem., Int. Ed.*, 2008, 47, 906.
50. Z. Xu, C. Li, Z. Hou, C. Peng and J. Lin, *Cryst. Eng. Comm.*, 2011, 13, 474.
51. J. Yang, C. Zhang, C. Li, Y. Yu and J. Lin, *Inorg. Chem*., 2008, 47, 7262.
52. Y. Zheng, H. You, K. Liu, Y. Song, G. Jia, Y. Huang, M. Yang, L. Zhang and G. Ning, *Cryst. Eng. Comm*., 2011, 13, 3001.
53. Z. Hou, Z. Cheng, G. Li, W. Wang, C. Peng, C. Li, P. Ma, D. Yang, X. Kang and J. Lin, *Nanoscale*, 2011, 3, 1568.
54. S. Huang, X. Zhang, L. Wang, L. Bai, J. Xu, C. Li and P. Yang, *Dalton Trans*., 2012, 41, 5634.
55. J. A. Dorman, J. H. Choi, G. Kuzmanich and J. P. Chang, *J. Phys. Chem. C*, 2012, 116, 12854.
56. X. Zhang, P. Yang, C. Li, D. Wang, J. Xu, S. Gai and J. Lin, *Chem. Commun*., 2011, 47, 12143.
57. F. Wang and X. Liu, *J. Am. Chem. Soc*., 2008, 130, 5642.

ISBN: 978-93-95369-55-8 (paperback) 978-93-95369-46-6 (electronic)

58. R. Kumar, M. Nyk, T. Y. Ohulchanskyy, C. A. Flask and P. N. Prasad, *Adv. Funct. Mater*., 2009, 19, 853.

59. H. Qiu, G. Chen, R. Fan, C. Cheng, S. Hao, D. Chen and C. Yang, *Chem. Commun*., 2011, 47, 9648.

60. H. Guo, N. Dong, M. Yin, W. Zhang, L. Lou and S. Xia, *J. Phys. Chem. B*, 2004, 108, 19205.

61. A. Patra, C. S. Friend, R. Kapoor and P. N. Prasad, *J. Phys. Chem. B*, 2002, 106, 1909.

62. A. Patra, C. S. Friend, R. Kapoor and P. N. Prasad, *Chem. Mater*., 2003, 15, 3650.

63. D. Geng, G. Li, M. Shang, C. Peng, Y. Zhang, Z. Cheng and J. Lin, *Dalton Trans*., 2012, 41, 3078.

64. X. Liu, L. Yan and J. Lin, *J. Phys. Chem*., C 2009, 113, 8478.

65. X. Liu, C. Li, Z. Quan, Z. Cheng and J. Lin, *J. Phys. Chem. C*, 2007, 111, 16601.

66. M. Yu, J. Lin and J. Fang, *Chem. Mater*., 2005, 17, 1783.

67. H. Wang, M. Yu, C. Lin, X. Liu and J. Lin, *J. Phys. Chem. C* 2007, 111, 11223; J. -P. Ge, W. Chen, L. -P. Liu and Y. -D. Li, *Chem. Eur. J.*, 2006, 12, 6552.

68. C. Gabriel, S. Gabriel, E. H. Grant, B. S. J. Halstead and D. M. P. Mingos, *Chem. Soc. Rev*., 1998, 27, 213.

69. Y. Lei, M. Pang, W. Fan, J. Feng, S. Song, S. Dang and H. Zhang, *Dalton Trans.*, 2011, 40, 142.

70. M. Pang, D. Liu, Y. Lei, S. Song, J. Feng, W. Fan and H. Zhang, *Inorg. Chem.*, 2011, 50, 5327.

71. V. I.Pârvulescu and C.Hardacre, *Chem. Rev.*, 2007, 107, 2615.

72. D. D. Lovingood and G. F. Strouse, *Nano Lett.*, 2008, 8, 3394.

73. A. Taubert, *Acta Chim. Slov.*, 2005, 52, 168.

74. N. O. Nuñez, M. Ocaña, *Nanotechnology*, 2007, 18, 455606.

75. C. Zhang, J. Chen, Y. Zhou and D. Li, *J. Phys. Chem. C*, 2008, 112, 10083.

76. J. Chen, C. Guo, M. Wang, L. Huang, L. Wang, C. Mi, J. Li, X. Fang, C. Mao and S. Xu, *J. Mater. Chem.*, 2011, 21, 2632.

77. C. Li, P. Ma, P. Yang, Z. Xu, G. Li, D. Yang, C. Peng and J. Lin, *Cryst. Eng. Comm.*, 2011, 13, 1003.

78. F. Wang, Y. Zhang, X. Fan and M. Wang, *Nanotechnology,* 2006, 17, 1527.

79. L. Zhou, Z. Chen, K. Dong, M. Yin, J. Ren and X. Qu, *Biomaterials*, 2014, 35, 8694.

ISBN: 978-93-95369-55-8 (paperback) 978-93-95369-46-6 (electronic)

80. B. I. Kharisov, O. V. Kharissova and U. O. Méndez, Radiation Synthesis of Materials and Compounds. Boca Raton, FL: CRC Press; 2013

81. J. Belloni, *Catal. Today*, 2006, 113, 141.

82. J. Marignier, J. Belloni, M. Delcourt and J. Chevalier, *Nature*, 1985, 317, 344.

83. A. Henglein and D. Meisel, *Langmuir*, 1998, 14, 7392.

84. J. Biswal, S. P. Ramnani, R.Tewari, G. K. Dey and S. Sabharwal, *Radiat. Phys. Chem.*, 2010, 79, 441.

85. C. M. Doudna, M. F. Bertino, F. D. Blum, A. T. Tokuhiro, D. Lahiri-Dey, S. Chattopadhyay and J. Terry, *J. Phys. Chem. B*, 2003, 107*,* 2966.

86. Md R. Karim, K. T. Lim, C. J. Lee, Md T. Islam Bhuiyan, H. J. Kim, L. -S. Park, M. S. Lee, *J. Polym. Sci., Part A: Polym. Chem.*, 2007, 45, 5741.

87. Z. Zhang, T. M. Nenoff, K. Leung, S. R. Ferreira, J. Y. Huang, D. T. Berry, P. P. Provencio and R. Stumpf, *J. Phys. Chem. C*, 2010, 114, 14309.

88. V. Nagpala, A. D. Bokarea, R. C. Chikate, C. V. Rodec, K. M. Paknikara, *J. Hazard. Mater.*, 2010, 175, 680.

89. A. Chatterjee, A. Priyam, S. K. Das and A. Saha, *J. Colloid Interface Sci.*, 2006, 294, 334.

90. N. Keghouchea, S. Chettibia, F. Latrechea, M. M. Bettaharb, J. Bellonic, J. L. Marignier, *Radiat. Phys. Chem.*, 2005, 74, 185.

91. J. F. Hund, M. F. Bertino, G. Zhang, C. S. -Leventis, N. Leventis, A. T. Tokuhiro and John Farmer, *J. Phys. Chem. B*, 2003, 107, 465.

92. V. Cuba, J. Indrei, V. Múčka, Martin Nikl, Alena Beitlerová, Milan Pospísil, Ivo Jakubec, *Radiat. Phys. Chem.*, 2011, 80, 957.

93. J. Barta, V. Cuba, M. Pospísil, V. Jary and Martin Nikl, *J. Mater. Chem.*, 2012, 22, 16590.

94. J. T. G. Overbeek, Colloidal Dispersions, J. W. Goodwin (ed.), Royal Society of Chemistry, London, 1981, p:1.

95. A. J. Bards, L. R. Faulkner, *Electrochemical methods-Fundamentals and Applications*, John Wiley & Sons, New York, 1980.

96. P. Somasundaran, B. Markovic, S. Krisnakumar and X. Yu, *Handbook of Surface and Colloidal Chemistry*, CRC Press, Boca Raton, FL, 1997, P:559.

97. Y. Zhang, Y. Tang, X. Liu, L. Zhang and Y. Lv, *Sens. Actuators, B*, 2013, 185, 363.

98. J. Peng, Y. Wang, J. Wang, X. Zhou and Z. Liu, *Biosens. Bioelectron.*, 2011, 28, 414.

ISBN: 978-93-95369-55-8 (paperback) 978-93-95369-46-6 (electronic)

99. R. Arppe, I. Hyppänen, Perälä, N., M. Schäferling, and T. Soukka, *Nanoscale*, 2015. *7*, 27, 11746-11757

100. B. Chen, and F., Wang, *Accounts of Chemical Research*, 2019, *53*, 2, 358-367.

101. T.K., Rezende, H.P. Barbosa, L.F. Dos Santos, K. de O. Lima, P. Alves de Matos, T.M. Tsubone, R.R. Gonçalves, and J.L., Ferrari, *Frontiers in Chemistry*, 2022, 10,1035449.

102. S., Hao, G. Chen, and C. Yang, *Theranostics* 2013, *3*5, 331.

103. T. J, Akkewar, N. R, Baig and S. J. Dhoble. *Oriental Jornal of Physical Sciences* 2025; 10, 1.

104. M. Wang, Li, M A x. Yu, J, Wu, and C. Mao, *ACS applied materials & interfaces*, 2015, *7*51, 28110-28115.

105. H. Huang, and J.J., Zhu, 2019. *Analyst*, *144*, 23, pp.6789-6811.

106. Z. Chen, X. Zhou, M. Mo, X. Hu, J. Liu, and L. Chen, *Journal of Nanobiotechnology*, 2024, 22, 185.

107. M. Bai, H. Wan, Y. Zhang, S., Chen, C. Lu, X. Liu, G. Chen, N, Zhang, and R. Ma, *Chemical Science*. 2024.

108. Q. Li, H. Rao, H. Mei, Z. Zhao, W. Gong, A. Camposeo, D. Pisignano, and X. Yang, *Advanced Materials Interfaces*, 2022, *9*, 24, 2201175.

109. S. Gupta, *Handbook on the Physics and Chemistry of Rare Earths*, 2023, *63*, 99-140.

ISBN: 978-93-95369-55-8 (paperback) 978-93-95369-46-6 (electronic)